ELSEVIER

International Journal of Mass Spectrometry 220 (2002) 331–341

International Journal of Mass Spectrometry

www.elsevier.com/locate/ijms

Reactions of hydrated aluminum ions with methanol and formic acid

O. Petru Balaj [a], Edmond P.F. Lee [b], Iulia Balteanu [a], Brigitte S. Fox [a], Martin K. Beyer [a,1], John M. Dyke [b,2], Vladimir E. Bondybey [a,*]

[a] *Institut für Physikalische und Theoretische Chemie, Technische Universität München, Lichtenbergstraße 4, 85747 Garching, Germany*
[b] *Department of Chemistry, University of Southampton, Highfield, Southampton SO17 1BJ, UK*

Received 27 December 2001; accepted 18 March 2002

Abstract

The reactions of hydrated aluminum ions $Al(H_2O)_n^+$, $20 < n < 60$, with methanol and formic acid were investigated using Fourier transform ion cyclotron resonance (FT-ICR) mass spectrometry. Besides black body radiation and collisionally induced fragmentation, also efficient ligand transfer processes as well as an intracluster oxidation of the aluminum take place. While in pure $Al(H_2O)_n^+$ ions this reaction, where the Al^+ is oxidized to Al^{3+} and water reduced to yield molecular H_2, proceeds only in a limited size range of $11 < n < 24$. Addition of formic acid, similar to the previously studied addition of HCl, removes the upper limit, but the reactions proceed more slowly. With methanol, the upper limit remains, but it is shifted to higher values of n. These observations are consistent with our previously proposed "acid catalyzed", concerted proton transfer mechanism, with the efficiency of the reaction being highest in the presence of HCl, and decreasing with the decreasing acidities of formic acid and methanol. (Int J Mass Spectrom 220 (2002) 331–341)

Keywords: Hydrated aluminum ion; Methanol; Formic acid; Redox reactions; Hydrogen formation

1. Introduction

In the course of the last few years we have used an efficient cluster source developed in our laboratory to study the behavior of a large variety of hydrated ions [1–9]. The source can generate both anions and cations solvated with up to over 100 water molecules or other ligands, which can be transferred into and stored under ultra-high vacuum in an electromagnetic FT-ICR trap. The stored clusters gradually fragment due to absorption of the infrared background radiation [1,9–12] and collisions, if a reaction gas is present [1–3]. Investigations of hydrated aluminum cations, $Al(H_2O)_n^+$ have revealed, in addition to fragmentation, also an interesting, exothermic intracluster reaction, in which the aluminum is oxidized yielding an Al^{3+} hydroxide and simultaneously reducing water, with molecular H_2 being released, and water molecules evaporating from the cluster. Interestingly, the reaction only proceeded over a limited size range, in clusters with 11–25 water ligands:

$$Al^+(H_2O)_n \rightarrow Al(OH)_2^+(H_2O)_{n-m-2} + H_2 + mH_2O, \quad 11 \leq n \leq 25,\ m = 2, 3$$

It should be emphasized, that the hydrated Al^+ clusters are formed in the source, with the reaction

* Corresponding author. E-mail: bondybey@ch.tum.de
[1] Co-corresponding author. E-mail: beyer@ch.tum.de
[2] Co-corresponding author. E-mail: jmdyke@soton.ac.uk

1387-3806/02/$ – see front matter
PII S1387-3806(02)00686-3

taking place hundreds of milliseconds later, in the high vacuum, collision-free environment of the FT-ICR instrument, activated simply by the 300 K background infrared radiation. We have proposed two possible mechanisms for this reaction, an insertion of the aluminum into an O–H bond, and a concerted proton transfer [1].

Similar hydrogen elimination processes in metal-solvent clusters have now also been observed in molecular beam experiments in a number of different circumstances. In one of these experiments, H_2 is formed when water clusters containing at least three sodium atoms are ionized [13–15]. Formation of $Mg(OH)^+(H_2O)_n$ hydroxide was observed in collisions of the monovalent alkaline earth metal ions, Mg^+ (or Ca^+) with neutral water clusters [16–20]. Similar hydrogen loss was observed with methanol [21–24], and ethanol [25], as recently reviewed by Fuke et al. [26], and in some cases, even methyl radicals are formed, as in Mg^+ solvated with dimethyl ether [27] and Sr^+ with methanol [21]. Also small hydrated aluminum ions have been previously studied both experimentally [28] and by theory [29], but no intracluster reactions were reported.

To clarify the mechanism of the intracluster reaction, we have carried out additional experiments, "dissolving" gaseous hydrogen chloride in the hydrated clusters [2]. As soon as a molecule of hydrogen chloride is taken up by the cluster, the intracluster reduction–oxidation reaction and formation of molecular hydrogen proceeds, and the upper size limit disappears:

$$Al^+(H_2O)_n + HCl \rightarrow Al(OH)Cl^+(H_2O)_p + H_2 + qH_2O, \quad 11 \leq n,\ p + q = n - 1$$

The lower size limit $n = 11$ is, on the other hand, retained. It was shown previously that the hydrogen chloride dissolves in the cluster ionically [30–37], with at least 11 water molecules being needed for the HCl to dissolve, and the hydrated H^+ and Cl^- ions to form. This observation, that the hydrogen formation is promoted by the introduction of a proton into the cluster, provides a strong support for the proton transfer mechanism we have previously proposed [2]. In a number of theoretical works by several different authors it was recently found that a concerted proton transfers through a water chain can significantly reduce the activation energy of a reaction [38–43].

In the present manuscript we explore the question, to what extent can the proton transfer and the hydrogen evolution be fine-tuned by the introduction of various reactants, such as methanol or formic acid, with acidities intermediate between those of water and hydrogen chloride. The effect of these reactants on the hydrogen formation reaction could thus give further insight, and support for or against the proton transfer mechanism. In this manuscript we report our findings and their interpretation with supporting high-level ab initio quantum mechanical calculations.

2. Experimental and computational details

2.1. Experimental procedure

The experiments were performed on a modified FT-ICR mass spectrometer Bruker/Spectroscopin CMS47X [44], equipped with a superconducting 4.7 T magnet and a cylindrical 60 mm × 60 mm "infinity" cell. The cations were produced by laser vaporization of a rotating target disk made from aluminum (Aldrich, ≥99%). The plasma is entrained by a carrier gas pulse, in our case helium seeded with water, supplied by a home-built piezoelectric valve with a 50 μs opening time, and cooled by flowing through a confining channel. Aluminum cations solvated by water are formed in the subsequent adiabatic expansion into vacuum where they are accelerated, and further guided by electrostatic lenses. They are transferred through four stages of differential pumping and finally decelerated and stored in the ICR cell, with a base pressure of $\sim 4 \times 10^{-10}$ mbar.

The temperature of the trapped cluster ions is determined by a competition between evaporative cooling and radiative heating by the ambient temperature background radiation [9,45]. To study the cluster chemistry, the reactants, in the present case, formic acid (Aldrich 99%) and methanol (Aldrich 99%), were

introduced into the ultra high vacuum region through a needle valve to raise the pressure to a desired value, typically 5×10^{-8} mbar in the present experiments. Mass spectra were taken at the completion of ion accumulation, and then after different reaction delays to monitor the progress of the reaction.

2.2. Theoretical methods

Ab initio calculations have been carried out on the hydrogen elimination reactions, $Al^+(AH)(BH) \rightarrow AlAB^+ + H_2$, for A, B = OH, CH_3O, and HCOO, using the Gaussian 98 [46] program. For all the species involved, the geometry was optimized with the MP2 method using the 6-311G(2d,2p) basis set. With the optimized geometry, thermochemical constants were computed using the G2 and the RCCSD(T) methods. The calculations do not take into account the effects of solvation.

In all cases it was intended to evaluate thermodynamic constants at the G2 level, but it was not possible to complete the calculations with this method for $Al(OH)_2{}^+$, because the HF/6-31G* geometry of this ion was near linear and the MP2(full)/6-31G* geometry optimization did not converge. Because of this, the RCCSD(T)/aug-cc-pVTZ//MP2/6-311++ G(2d,2p) relative energies, the MP2/6-311++G(2d,2p) geometries and vibrational frequencies were used for the case A = OH, B = OH to evaluate the reaction thermodynamic constants, instead of the G2 method. The RCCSD(T)/aug-cc-pVTZ//MP2/6-311++ G(2d,2p) level is higher than the QCISD/6-311++G(3df,2p) level, which is the target of the composite method, G2. For some of the reactions considered, both the G2 and RCCSD(T)//MP2 levels of calculation were employed to evaluate their thermodynamic constants.

3. Results and discussion

3.1. Reactions of $Al^+(H_2O)_n$ with methanol CH_3OH

Fig. 1 exemplifies a typical initial distribution of clusters at a nominal time $t = 0$. Since the reactions and ligand exchange can occur already during the ion accumulation, one observes here not only the hydrated Al^+ ion reactants (connected by the dotted line), but also some primary (dashed line) and even secondary products (longer dashes). The initial distribution here ranges from 20 to about 60 water ligands, with a maximum intensity around $n \approx 37$. The reaction proceeds through a basically thermoneutral ligand exchange of water molecules for CH_3OH:

$$Al^+(H_2O)_n(CH_3OH)_m + CH_3OH \rightarrow Al^+(H_2O)_{n-k}(CH_3OH)_{m+1} + kH_2O, \quad k \approx 1$$

Note the oscillations in the initial reactant cluster distribution around the intensity maximum, with the $n = 33$, 35, 37, and 39 clusters exhibiting appreciably higher intensities than the intervening $n = 34$, 36, and 38 species. The same pattern appears to be repeated in the primary product distribution, but shifted to higher masses by 14 amu, the difference between the masses of methanol and water ligands, 32 and 18 amu, respectively, and a hint of the structure is observable even in the secondary exchange product. This suggests that the initial ligand exchange is extremely efficient, and competitive with the cluster fragmentation.

The initial stages of the reaction can be seen more clearly in Fig. 2, which shows two sections of the mass spectra at higher resolution, at a nominal delay of 0 s, as well as after 0.7 and 1.5 s. At the right-hand side the region of larger $Al^+(H_2O)_n$ clusters, in the range of about $n = 35$–37 is shown. Already at the nominal $t = 0$ ligand exchange products containing 1–3 methanol molecules can be seen, due to reactions occurring during the accumulation process. To the left of the peak labeled m, n = 0,37, i.e., cluster with 37 water and 0 methanol ligands, appear peaks shifted by 4 and 8 amu to lower masses, which correspond to the m, n = 1,35 and m, n = 2,33 species. The exchange products with $m$$CH_3OH$ ligands will be shifted $4m$ amu to lower mass with respect to the hydrated Al^+ clusters, corresponding to the difference between the mass of two molecules of water, 36 amu, and that of methanol, 32 amu. In the two spectra at longer time delays one can observe that the reaction proceeds further, with

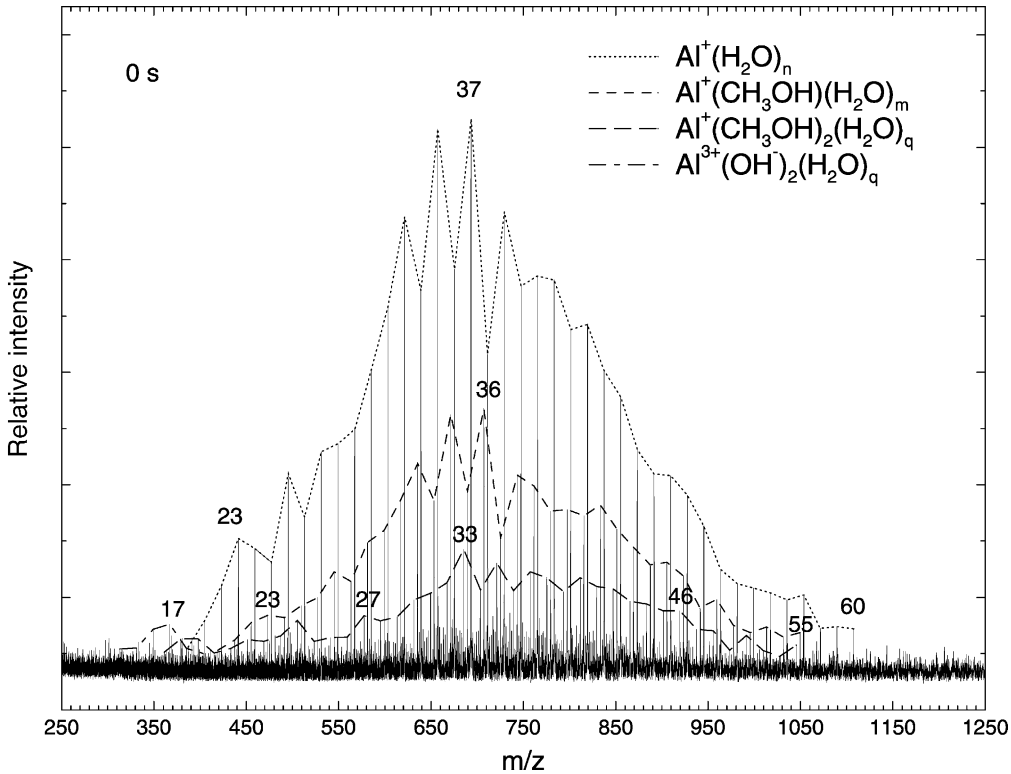

Fig. 1. Mass spectrum of the initial cluster distribution $Al^+(H_2O)_n$, $n = 20$–60, for methanol reactions, with a nominal reaction delay of 0 s, after accumulating the ions for 2 s in the ICR-cell. The reactions proceed through ligand exchange. Up to two methanol molecules have already been taken up by the clusters.

the distribution maximum shifting to clusters with 2 and 4 methanol ligands after 0.7 and 1.5 s, respectively.

On the left-hand side of the figure, a distribution of smaller clusters, in the range of $n = 28$–30 is shown. In this case, however, one can see in the 0.7 and 1.5 s panels that major products are not shifted $4m$, i.e., 4, 8, 12, ... amu from the pure hydrated Al^+ clusters, but $4m + 2$ amu, i.e., 2, 6, 10, ... amu. As previously observed with pure hydrated aluminum ions [1,2], the ligand exchange is again accompanied by an intracluster reaction leading to the oxidation of aluminum to Al^{3+} forming aluminum hydroxide, while reducing hydrogen and eliminating molecular H_2:

$$Al^+(H_2O)_n(CH_3OH)_m \rightarrow Al(OH)(CH_3O)^+(H_2O)_{n-p} + H_2 + (p-1)H_2O, \quad m = 1$$

$$Al^+(H_2O)_n(CH_3OH)_m \rightarrow Al(CH_3O)_2{}^+(H_2O)_{n-p}(CH_3OH)_{m-2} + H_2 + pH_2O, \quad m \geq 2$$

Compared to the pure $Al^+(H_2O)_n$ where the reaction does not occur in clusters with $n > 24$, however, the upper limit appears to be shifted to a somewhat higher value of n.

The exchange does not stop at one or two methanol ligands, but continues further, and there seems to be no apparent upper limit for the number of methanol molecules which can be taken up by the cluster. Its rate, however, slows down considerably above $m \approx 5$, while the fragmentation continues. After 5 s, the largest clusters are $Al(CH_3O)_2{}^+(CH_3OH)_{13}(H_2O)_6$. The smallest cluster observed in this experiment which contains only methanol is, after 10 s,

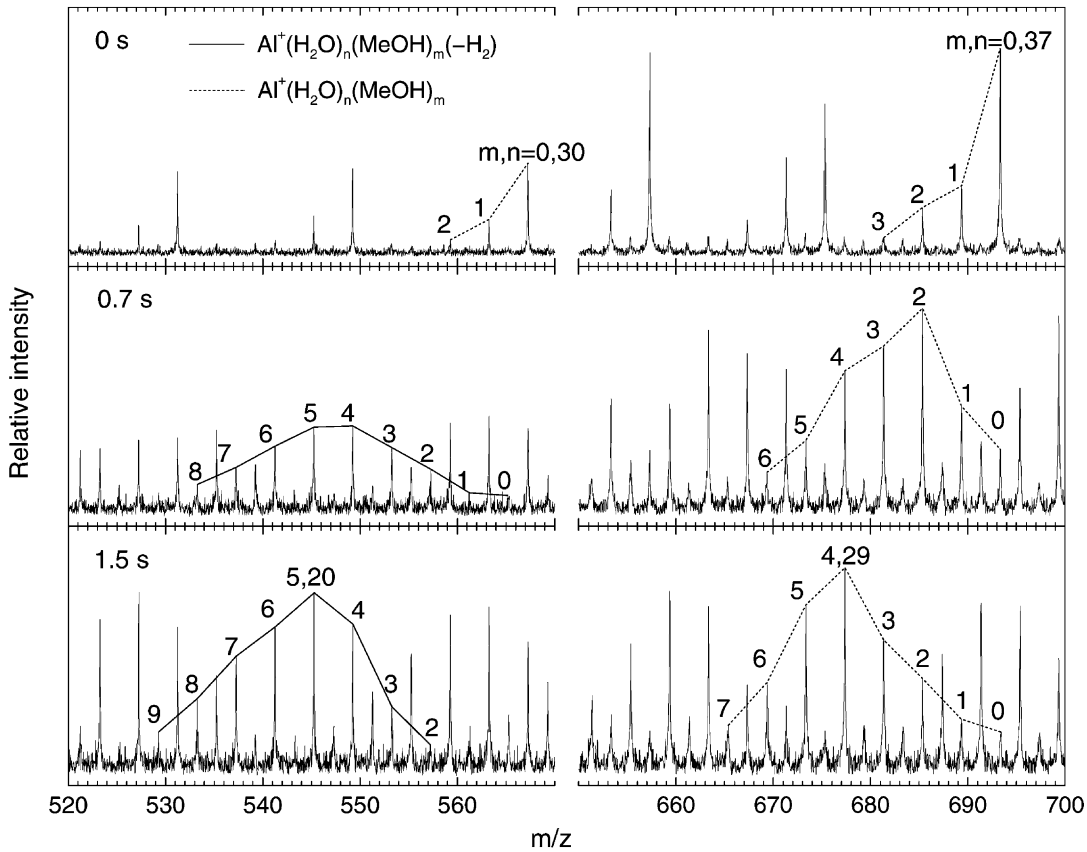

Fig. 2. Representative sections of mass spectra illustrating the upper size limit for the intracluster reaction in the ligand exchange reaction with methanol. The peaks are labelled indicating the number of methanol molecules in the corresponding cluster. At 0 s, no hydrogen elimination product is present both on the left and right sides. At longer times, exemplified at 0.7 and 1.5 s, the ligand exchange pattern on the right side corresponding to larger clusters develops in time, while on the left side, displaying clusters containing less than 30 solvent molecules, H_2 elimination shifts the peak group by 2 amu. The exact transition between these two regions is blurred, but the existence of an upper size limit around a total of 30 solvent molecules can unambiguously be established.

$Al(CH_3O)_2{}^+(CH_3OH)_7$. After 80 s essentially only two "final" cluster products remain, $Al(CH_3O)_2{}^+(CH_3OH)_2$ and $Al(CH_3O)_2{}^+(CH_3OH)_3$.

The initial cluster distributions contains, besides the hydrated aluminum clusters, also trace amounts of a whole range of hydrated proton clusters, $H^+(H_2O)_n$. These also exchange water for methanol, and since in the end the entire distribution is converted to a single product cluster, $H^+(CH_3OH)_4$, this becomes clearly observable among the final products.

Since all the major end-products contain Al^{3+} with two methanolate anions, $Al^{3+}(CH_3O^-)_2$, even though in the initial stages of the reaction also $Al(OH)_2{}^+(H_2O)_n$ ions were produced, clearly also the hydroxides were replaced by methanolate. There is therefore some ambiguity as to the true structure of some of the early products which can be either formulated as $Al(CH_3O)_2{}^+(H_2O)_{n-p}(CH_3OH)_{m-2}$, as shown in reaction (1), or alternatively as solvated hydroxides, $Al(OH)_2{}^+(H_2O)_{n-p-2}(CH_3OH)_m$. The total absence of hydroxides among the final products suggests that any hydroxide ions are presumably replaced by methanolate shortly after a methanol molecule enters the cluster, and also our accompanying ab

initio calculations discussed in Section 3.3 seem to favor the methanolate structure.

3.2. Reactions of $Al^+(H_2O)_n$ with formic acid

Fig. 3 shows mass spectra of the cluster distribution after 0.3 and 1 s reaction time with formic acid. The clusters $Al^+(H_2O)_n$, $n = 17$–57, again exhibit fragmentation and ligand exchange reactions which are, however, considerably slower than in the case of methanol. The intracluster reaction leading to the formation of molecular hydrogen is again observed, but the data analysis is somewhat complicated by the fact that clusters containing two formic acid molecules after the H_2 elimination, $Al(HCOO)_2{}^+(H_2O)_{n-5}$, have the same nominal mass as the initial $Al^+(H_2O)_n$ species. While in principle the mass resolution in FT-ICR should be adequate to distinguish these ions by their mass defect, this is not accomplished in broad-band mode in this mass range due to the limitations of the ASPECT3000 data station.

In spite of this difficulty, one can see clearly from Fig. 3 that over the entire cluster size range studied an efficient intracluster aluminum oxidation and molecular hydrogen elimination proceeds:

$$Al^+(H_2O)_n(HCOOH) \rightarrow Al(OH)(HCOO)^+(H_2O)_{n-p} + H_2 + (p-1)H_2O, \quad m = 1$$

At least up to about $n = 57$ the upper size limit seems to be removed by the presence of formic acid, similar to the case of HCl. Owing to the lower acidity of HCOOH as compared with HCl where the hydrogen elimination took place almost immediately, in the

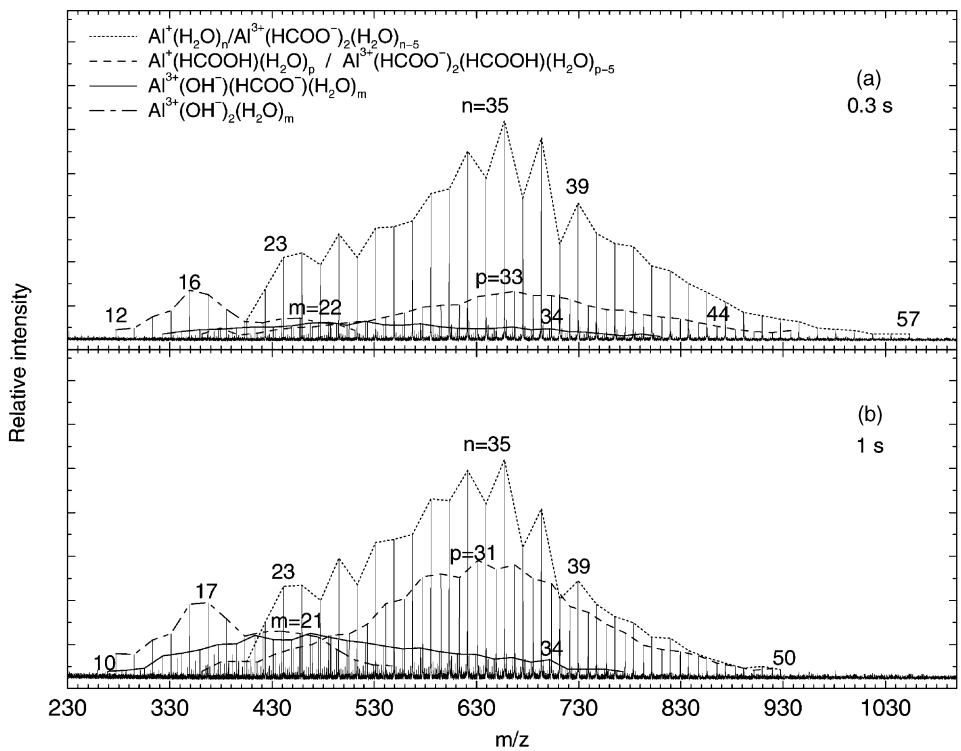

Fig. 3. Mass spectrum of the reaction of $Al^+(H_2O)_n$ with HCOOH formic acid after (a) 0.3 s and (b) 1 s. Due to the same nominal mass of $(H_2O)_5$ and $(HCOO)_2$ of 90 amu, clusters which have taken in two formic acid molecules and eliminated H_2 overlap with the initial cluster distribution, and subsequent exchange products also overlap, as indicated in the figure legend. The compared to methanol slower progress of ligand exchange and the elimination of H_2 without an upper size limit are clearly identified.

formic acid case the process seems to be at least an order of magnitude slower. One can clearly see in Fig. 3 both the ligand exchanged cluster prior to the H_2 elimination, as well as the Al^{3+} acetate–hydroxide product formed by the reduction–oxidation reaction. Apparently, the HCOOH molecule must first diffuse, on the time scale of the ICR experiment, through one or two solvent "layers", in order to get in contact with the central aluminum ion, and initiate the reaction.

In further collisions the remaining hydroxide anion can be replaced by $HCOO^-$ with the HCOOH proton recombining with OH^-:

$$Al(OH)(HCOO)^+(H_2O)_n + HCOOH \rightarrow Al(HCOO)_2{}^+(H_2O)_{n-m+1} + mH_2O$$

The lower overall rate of the exchange process is reflected in the smaller number of formic acid molecules taken up by the clusters. After about 5 s the largest number of formic acid ligands is in an $Al(HCOO)_2{}^+(HCOOH)_8(H_2O)_3$ cluster, while the smallest cluster containing only formic acid is $Al(HCOO)_2{}^+(HCOOH)_4$, observed after 10 s.

At the late stages of the reaction, also the formation of formic acid anhydride becomes feasible, leading to the elimination of an additional water molecule. The "final" dominant product remaining after 80 s is an $Al(HCOO)_2{}^+HCOOH((HCO)_2O)$ ion, which seems to be stable with respect to further fragmentation at room temperature, and which is apparently formed according to the reaction:

$$Al(HCOO)_2{}^+(HCOOH)_3 \rightarrow Al(HCOO)_2{}^+HCOOH((HCO)_2O) + H_2O$$

Apparently, formation of an anhydride from two formic acid molecules with the loss of water is favored, compared with the loss of an additional formic acid ligand. Like in the case of methanol, in the 80 s mass spectrum a final product of the reactions of the protonated water clusters with formic acid can again be found. The whole distribution of $H^+(H_2O)_n$ clusters initially present in trace amounts is now converted to a single product, the $H^+((HCO)_2O)_3$ cluster, a proton solvated by three formic acid anhydride molecules.

In all four cases studied, that is in pure $Al^+(H_2O)_n$, as well as in their reactions with HCl, HCOOH, and CH_3OH, the interesting hydrogen elimination can be rationalized with the previously suggested concerted proton transfer mechanism [1,2]. This is exemplified by the specific case of the HCOOH reaction in Fig. 4. It is initiated by the transfer of a proton originating from the formic acid molecule, which results in a transient formation of a hydroxonium cation in the second solvation shell of the Al^+. The s-electron pair of the Al^+ is then transferred outward, and the charge rearranged resulting in an $HCOO^-$–Al^{3+}–OH^- salt-bridge, with an H^-/H_3O^+ ion pair recombining to form H_2 and H_2O.

3.3. Theoretical results

To gain further insights into the mechanisms of molecular hydrogen elimination, we have carried out theoretical computations for reactions of the type:

$$Al^+(AH)(BH) \rightarrow Al(A)(B)^+ + H_2$$

Here AH, BH denote the Brönsted acids involved, i.e., H_2O, CH_3OH, or HCOOH, with the effect of the solvation shell not being explicitly considered. Although these reactions are fundamental for the redox chemistry of aluminum, to the best of our knowledge, they have not appeared in the literature so far. The only studies available so far deal with neutral and singly charged hydrated aluminum by Iwata and coworkers [29,47], and Al^{3+}–water potentials have been derived computationally by Wasserman et al. [48]. Detailed studies are available by several groups on the problem of aluminum insertion into the water O–H bond [47,49,50], which involves change of the aluminum oxidation state from +1 to +3, but H_2 elimination from large clusters has yet to be computationally treated. Our most recent results on competing H and H_2 elimination from hydrated vanadium ions $V^+(H_2O)_n$ [51] might prove to be an even bigger challenge for theory.

We initially intended to carry out the evaluation of all the thermodynamic constants at the G2 level, but encountered problems for some of the species, since

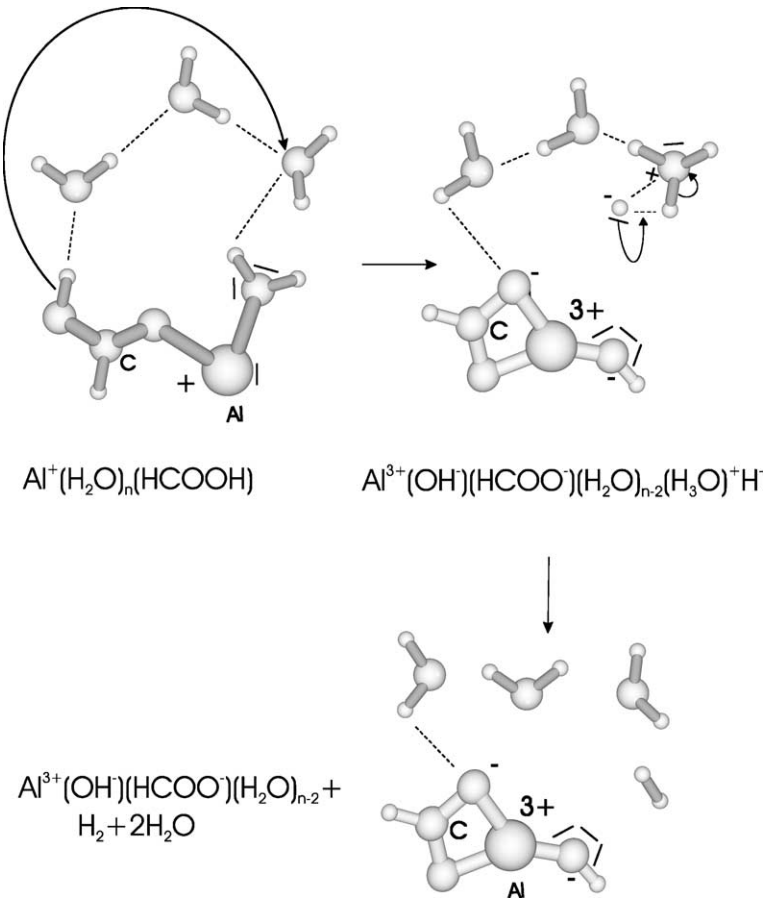

Fig. 4. Proposed mechanism of the intracluster reaction exemplified in an $Al^+(HCOOH)(H_2O)_n$ cluster. Dissolving formic acid results in a proton transfer and charge separation into H_3O^+ and $HCOO^-$ in the cluster. $HCOO^-$ comes in contact with the Al^+ ion inducing the shift of the $3s^2$ lone pair, which results in the $HCOO^-$–Al^{3+}–OH^- salt bridge and the formal H^-–H_3O^+ ion pair. By recombination, molecular hydrogen is formed and additional water molecules are lost. The aluminum ion is assumed as hexacoordinated with additional chains of water molecules between the first shell ligands. For clarity only the first hydration shell is shown in detail.

the HF/6-31G* geometry of $Al(OH)_2^+$ is nearly linear, and the MP2(full)/6-31G* geometry optimization failed to converge even after 60 cycles. Because of this, we have used RCCSD(T)/aug-cc-pVTZ relative energies, the MP2/6-311++G(2d,2p) geometries and vibrational frequencies to evaluate them instead. The RCCSD(T)/aug-cc-pVTZ//MP2/6-311++G(2d,2p) level is, in fact, higher than the QCISD/6-311++G(3df,2p) level, which is the target of the composite G2 level.

The changes in electronic energy for the hydrogen elimination reactions computed at different levels of correlation with the aug-cc-pVTZ basis are summarized in Table 1. The results suggest that the MP2 level is inadequate, but that the contribution from triple excitations is negligibly small. This suggests that if the assumption of additivity in the G2 method is valid, it is probably adequate for this type of reaction.

The thermodynamic constants obtained at the RCCSD(T)/aug-cc-pVTZ//MP2/6-311++G(2d,2p)

Table 1
The computed electronic energy changes for the title reaction with the aug-cc-pVTZ basis set at different levels of correlation

Reaction	Level	ΔE_e (kcal/mol)
$Al^+(H_2O)_2 \rightarrow Al^+(OH)_2 + H_2$	MP2	5.98
	CCSD	11.69
	CCSD(T)	11.53
$(CH_3OH)Al^+(H_2O) \rightarrow (CH_3O)Al^+(OH) + H_2$	MP2	4.88
	CCSD	10.66
	CCSD(T)	10.77
$(HCO_2H)Al^+(H_2O) \rightarrow (HCO_2)Al^+(OH) + H_2$	MP2	−13.6
	CCSD	−8.0
	RCCSD(T)	−8.5

level, within the harmonic oscillator rigid rotor approximation employing RCCSD(T) D_e values, MP2 optimized geometries and harmonic vibrational frequencies are shown in Table 2, together with the corresponding G2 values where they could be computed. The results show that in the case of water, i.e., A = B = OH, the computed electronic energy change of the reaction is positive. The zero-point energy correction reduces the energy change somewhat, with the reaction remaining slightly endothermic both at 0 and 289 K. A positive reaction entropy results then overall in a negative free energy change.

In the presence of one methanol molecule, i.e., A = CH_3O, B = HO, calculations could be carried out at both levels of theory, and allow an assessment of the reliability of the G2 level for this type of reactions. The differences between the G2 and RCCSD(T)//MP2 results may be considered as small, with the difference in the enthalpies being <3 kcal/mol. The differences in the computed entropy changes are <6 cal/(mol K), and in directions which make them cancel out each other in the evaluation of the Gibbs free energy. These differences lead overall to a very small difference of ca. 1 kcal/mol at 298 K in the Gibbs free energies computed at the two levels. The given entropy change at the G2 level is based on the scaled HF/6-31G* vibrational frequencies and optimized geometrical parameters. Similarly, small differences in the computed enthalpies and Gibbs free energies are found when one formic acid molecule is involved, A = HCOO, B = HO. In this case the difference in the computed enthalpy changes obtained at the two levels of calculation is <1.8 kcal/mol, the computed entropy changes <2 cal/mol K at 298 K.

Table 2 reveals that all the reactions considered are thermodynamically possible. The most favorable conditions occur when at least one formic acid molecule is involved, and also the presence of methanol favors the hydrogen elimination reaction slightly compared with pure hydrated aluminum clusters. The calculations thus support the experimental observation that an increasing acidity of the reactant favors the intracluster hydrogen elimination, which occurs fastest with formic acid, followed by methanol, and is least favored in pure hydrated aluminum clusters.

The presence of solvent molecules is surely expected to change the thermochemistry of the intracluster reaction considerably in favor of the products. The interaction energies of the solvent with the products, containing a triply charged Al^{3+} and two singly

Table 2
Summary of the computed thermodynamic constants (in kcal/mol) obtained at the G2 and RCCSD(T)/aug-cc-pVTZ//MP2/6-311++G(2d,2p) levels of theory, for the reactions: $Al^+(AH)(BH) \rightarrow Al^+(A)(B) + H_2$

Level	AH, BH	ΔH (0 K)	ΔH (298 K)	ΔG (298 K)
RCCSD(T)//MP2	H_2O, H_2O	2.9	4.4	−2.9
G2	H_2O, CH_3OH	0.3	1.5	−5.2
RCCSD(T)//MP2	H_2O, CH_3OH	2.7	4.2	−4.3
G2	CH_3OH, CH_3OH	0.6	1.9	−5.8
G2	HCOOH, HCOOH	−38.7	−38.5	−41.6
G2	H_2O, HCOOH	−17.9	−17.0	−23.1
RCCSD(T)//MP2	H_2O, HCOOH	−16.2	−15.5	−21.3

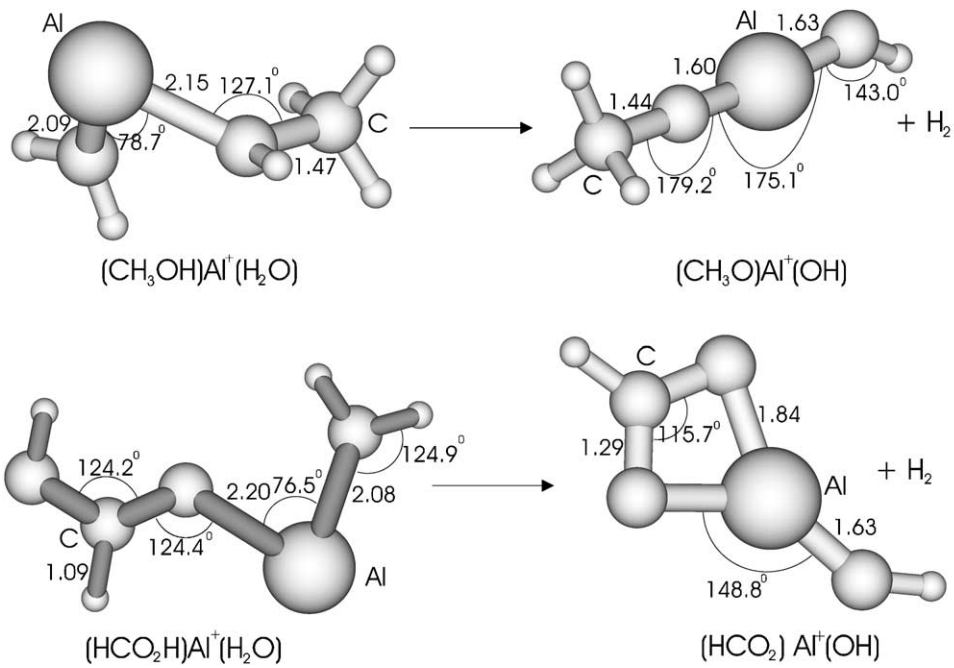

Fig. 5. Selected optimized geometries for hydrogen elimination reaction. The Al^{3+} compounds prefer a linear structure due to the negative charge of the ligands. Also the bond lengths shrink due to increased attraction between the negatively charged oxygen atoms and the Al^{3+} ion.

charged anions, are significantly enhanced over the initial singly charged Al^+, and the slightly positive enthalpy of some of the calculated reactions is very likely turned negative already by the addition of a single solvent molecule.

The calculated structures, exemplified in Fig. 5, reflect the loss of the hydrogen molecule, with the Al–O bond length shrinking in both reactions shown, a consequence of the 3+ charge on the aluminum atom after oxidation. Also interesting are the linear structures of the compounds containing Al^{3+}. The conformational change is induced by the negative charges of the oxygen atoms directly coordinated to Al^{3+}, which result in ligand repulsion.

4. Conclusions

The reaction of hydrated aluminum cations containing up to 60 water molecules with methanol and formic acid were studied. In both cases an efficient ligand exchange is followed by an intracluster reaction oxidizing the aluminum atom, thereby eliminating molecular hydrogen. The observed trend of the reaction rate, which increases with the acidity of the reactant, from pure water over CH_3OH, HCOOH to HCl provides a strong support for the previously proposed proton transfer mechanism of the reaction. The theoretical computations agree with this interpretation, the reaction enthalpies follow the same trend.

Acknowledgements

Financial support from the European Union through the Research Training Network “Reactive Intermediates”, the Deutsche Forschungsgemeinschaft, the Fonds der Chemischen Industrie, and the Leonhard-Lorenz-Stiftung (M.K.B.) is gratefully acknowledged.

References

[1] M. Beyer, C. Berg, W. Görlitzer, T. Schindler, U. Achatz, G. Albert, G. Niedner-Schatteburg, V.E. Bondybey, J. Am. Chem. Soc. 118 (1996) 7386.
[2] M. Beyer, U. Achatz, C. Berg, S. Joos, G. Niedner-Schatteburg, V.E. Bondybey, J. Phys. Chem. A 103 (1999) 671.
[3] C. Berg, U. Achatz, M. Beyer, S. Joos, G. Albert, T. Schindler, G. Niedner-Schatteburg, V.E. Bondybey, Int. J. Mass Spectrom. Ion Process. 167/168 (1997) 723.
[4] C. Berg, M. Beyer, U. Achatz, S. Joos, G. Niedner-Schatteburg, V.E. Bondybey, Chem. Phys. 239 (1998) 379.
[5] U. Achatz, S. Joos, C. Berg, M. Beyer, G. Niedner-Schatteburg, V.E. Bondybey, Chem. Phys. Lett. 291 (1998) 459.
[6] U. Achatz, B.S. Fox, M.K. Beyer, V.E. Bondybey, J. Am. Chem. Soc. 123 (2001) 6151.
[7] B.S. Fox, M.K. Beyer, U. Achatz, S. Joos, G. Niedner-Schatteburg, V.E. Bondybey, J. Phys. Chem. A 104 (2000) 1147.
[8] T. Schindler, C. Berg, G. Niedner-Schatteburg, V.E. Bondybey, Chem. Phys. 201 (1995) 491.
[9] T. Schindler, C. Berg, G. Niedner-Schatteburg, V.E. Bondybey, Chem. Phys. Lett. 250 (1996) 301.
[10] R.C. Dunbar, T.B. McMahon, Science 279 (1998) 194.
[11] M. Sena, J.M. Riveros, Rapid Commun. Mass Spectrom. 8 (1994) 1031.
[12] P.D. Schnier, W.D. Price, R.A. Jockusch, E.R. Williams, J. Am. Chem. Soc. 118 (1996) 7178.
[13] U. Buck, C. Steinbach, J. Phys. Chem. A 102 (1998) 7333.
[14] C.J. Mundy, J. Hutter, M. Parrinello, J. Am. Chem. Soc. 122 (2000) 4837.
[15] F. Mercuri, C.J. Mundy, M. Parrinello, J. Phys. Chem. A 105 (2001) 8423.
[16] K. Fuke, F. Misaizu, M. Sanekata, K. Tsukamato, S. Iwata, Z. Phys. D 26 (1993) S180.
[17] A.C. Harms, S.N. Khanna, B. Chen, A.W. Castleman, J. Chem. Phys. 100 (1994) 3540.
[18] H. Watanabe, S. Iwata, K. Hashimoto, F. Misaizu, K. Fuke, J. Am. Chem. Soc. 117 (1995) 755.
[19] M. Sanekata, F. Misaizu, K. Fuke, J. Chem. Phys. 104 (1996) 9768.
[20] D.C. Sperry, A.J. Midey, J.I. Lee, J. Qian, J.M. Farrar, J. Chem. Phys. 111 (1999) 8469.
[21] J. Qian, A.J. Midey, S.G. Donnelly, J.I. Lee, J.M. Farrar, Chem. Phys. Lett. 244 (1995) 414.
[22] C.A. Woodward, M.P. Dobson, A.J. Stace, J. Phys. Chem. A 101 (1997) 2279.
[23] W. Lu, S. Yang, J. Phys. Chem. A 102 (1998) 825.
[24] J.I. Lee, D.C. Sperry, J.M. Farrar, J. Chem. Phys. 114 (2001) 6180.
[25] N. Horimoto, J. Kohno, F. Mafuné, T. Kondow, J. Phys. Chem. A 103 (1999) 1518.
[26] K. Fuke, K. Hashimoto, S. Iwata, Adv. Chem. Phys. 110 (1999) 431.
[27] B. Soep, M. Elhanine, C.P. Schulz, Chem. Phys. Lett. 327 (2000) 365.
[28] F. Misaizu, M. Sanekata, K. Fuke, Z. Phys. D 26 (1993) S177.
[29] H. Watanabe, S. Iwata, J. Phys. Chem. 100 (1996) 3377.
[30] T. Schindler, C. Berg, G. Niedner-Schatteburg, V.E. Bondybey, Chem. Phys. Lett. 229 (1994) 57.
[31] C. Dedonder-Lardeux, G. Grégoire, C. Jouvet, S. Martrenchard, D. Solgadi, Chem. Rev. 100 (2000) 4023.
[32] R.S. MacTaylor, J.J. Gilligan, D.J. Moody, A.W. Castleman Jr., J. Phys. Chem. A 103 (1999) 4196.
[33] D. Laria, R. Kapral, D. Estrin, G. Ciccotti, J. Chem. Phys. 104 (1996) 6560.
[34] D. Estrin, J. Kohanoff, D. Laria, R.O. Weht, Chem. Phys. Lett. 280 (1997) 280.
[35] H. Arstila, K. Laasonen, A. Laaksonen, J. Chem. Phys. 108 (1998) 1031.
[36] I. Kusada, Z.G. Wang, J.H. Seinfeld, J. Chem. Phys. 108 (1998) 6829.
[37] S. Re, Y. Osamura, K. Morokuma, J. Phys. Chem. A 103 (1999) 3535.
[38] P.E.M. Siegbahn, J. Phys. Chem. 100 (1996) 14672.
[39] M.T. Nguyen, G. Raspoet, L.G. Vanquickenborne, P.T. van Duijnen, J. Phys. Chem. A 101 (1997) 7379.
[40] M. Aida, H. Yamataka, M. Dupuis, Chem. Phys. Lett. 292 (1998) 474.
[41] M. Aida, H. Yamataka, J. Mol. Struct.-Theochem. 462 (1999) 417.
[42] H. Yamataka, M. Aida, Chem. Phys. Lett. 289 (1998) 105.
[43] J. Andrés, M. Canle, M.V. García, L.F.R. Vázquez, J.A. Santaballa, Chem. Phys. Lett. 342 (2001) 405.
[44] C. Berg, T. Schindler, G. Niedner-Schatteburg, V.E. Bondybey, J. Chem. Phys. 102 (1995) 4870.
[45] B.S. Fox, M.K. Beyer, V.E. Bondybey, J. Phys. Chem. A 105 (2001) 6386.
[46] M.J. Frisch, G.W. Trucks, H.B. Schlegel, G.E. Scuseria, M.A. Robb, J.R. Cheeseman, V.G. Zakrzewski, J.A. Montgomery, Jr., R.E. Stratmann, J.C. Burant, S. Dapprich, J.M. Millam, A.D. Daniels, K.N. Kudin, M.C. Strain, O. Farkas, J. Tomasi, V. Barone, M. Cossi, R. Cammi, B. Mennucci, C. Pomelli, C. Adamo, S. Clifford, J. Ochterski, G.A. Petersson, P.Y. Ayala, Q. Cui, K. Morokuma, D.K. Malick, A.D. Rabuck, K. Raghavachari, J.B. Foresman, J. Cioslowski, J.V. Ortiz, A.G. Baboul, B.B. Stefanov, G. Liu, A. Liashenko, P. Piskorz, I. Komaromi, R. Gomperts, R.L. Martin, D.J. Fox, T. Keith, M.A. Al-Laham, C.Y. Peng, A. Nanayakkara, C. Gonzalez, M. Challacombe, P.M.W. Gill, B. Johnson, W. Chen, M.W. Wong, J.L. Andres, C. Gonzalez, M. Head-Gordon, E.S. Replogle, J.A. Pople, Gaussian 98, Revision A.7, Gaussian, Inc., Pittsburgh, PA, 1998.
[47] H. Watanabe, M. Aoki, S. Iwata, Bull. Chem. Soc. Jpn. 66 (1993) 3245.
[48] E. Wasserman, J.R. Rustad, S.S. Xantheas, J. Chem. Phys. 106 (1997) 9769.
[49] S. Sakaki, K.D. Jordan, J. Phys. Chem. 97 (1993) 8917.
[50] J. Hrušák, D. Stöckigt, H. Schwarz, Chem. Phys. Lett. 221 (1994) 518.
[51] B.S. Fox, I. Balteanu, O.P. Balaj, M.K. Beyer, V.E. Bondybey, Phys. Chem. Chem. Phys. 4 (2002) 2224.